TransCom 3 Final Report

Kevin Gurney[1], Peter Rayner[2], Rachel Law[2], Scott Denning[1] and the TransCom 3 modelers[3]

[1] Department of Atmospheric Science, Colorado State University, Fort Collins, CO, 80523, USA
[2] CSIRO Atmospheric Research, PMB 1, Aspendale, Victoria 3195, Australia
[3] A complete list of the TransCom 3 modelers is supplied in Appendix B.

1. Introduction

Much of our understanding of the global carbon budget is derived from atmospheric observations of CO_2. Hemispheric or regional fluxes may be calculated from atmospheric concentration measurements by a numerical procedure known as an "inversion," which requires that atmospheric transport be accounted for using a Chemical Tracer Model (Tarantola, 1987). However, there have traditionally been large differences between modeling approaches and results. For example, in a 1998 publication Songmiao Fan and colleagues at Princeton University found that most of the terrestrial uptake of atmospheric CO_2 is occurring in North America, and that this "sink" approximately balances fossil fuel emissions in the United States (Fan et al., 1998). Working with the same atmospheric data but using a different CTM and inversion method, Peter Rayner and colleagues at the Australian CSIRO found that the sink is distributed much more widely, with North America accounting for only a small fraction (Rayner et al., 1999).

Discrepancies such as these were the prime motivating force behind the TransCom 3 project. By involving inverse modelers from around the world into a collaborative experiment, it was anticipated that a deeper understanding of the factors that give rise to varying regional carbon flux estimates might be achieved. Furthermore, the process could serve to improve the methods used in inverse carbon cycle modeling. At the outset, the stated goals of the TransCom experiment were succinctly stated as follows:

(1) To quantify the degree of uncertainty in carbon budget inverse calculations that arises from CTM transport;

(2) Analyze the mechanisms by which the models differ; and

(3) Recommend and prioritize improvements to the observing and modeling systems to produce more robust carbon budget inversions in the future.

An experimental approach was designed to meet these objectives which contained three levels of participation (Gurney et al., 2000). The first level focused on annual mean carbon sources and sinks and required a limited number of tracers using supplied input fields of regional carbon exchange. The second level expanded on the first by including an inverse calculation of the strength of the seasonal cycle in regional fluxes, but required a much larger number of CTM tracers. The third level invited participants to perform their own inversions allowing for a comparison of different inversion methods. This last level is still ongoing.

Though the results of the TransCom 3 experiment continue to be analyzed, there is a general recognition within the inverse community that TransCom has met, and often surpassed, these modest initial goals (see Appendix A). As will be shown, the carbon flux estimates generated by the TransCom experiment are robust to details of the inversion set-up and data choices. Much of this is due to the participation of nearly all the research groups engaged in carbon cycle inverse modeling allowing for the computation of model mean flux estimates. As a result, TransCom has become a benchmark for work in this field and has resulted in greater communication and collaboration among those engaged in carbon cycle inverse modeling.

Sixteen transport models or transport model variants participated in the Level 1 TransCom 3 experiment while twelve models participated in the Level 2 experiment. The models ran forward simulations of a series of prepared regional and background global fluxes. The simulations were sampled following agreed upon

protocols and deposited centrally. CO_2 observations spanning the 1992 to 1996 time period were averaged from the Globalview dataset to serve as the observational data constraint to the inversion process. The process employed a Bayesian synthesis approach which specified prior fluxes and prior flux uncertainties for the 11 land and 11 ocean regions (Enting et al, 1995). The level 1 inversion produced annual mean flux estimates in these regions while the Level 2 produced estimates by region and calendar month.

2. Results

2.1 Annual mean carbon sources and sinks

2.1.1 Model mean results. Figure 1 shows the mean flux estimates (left X's in each box) and two uncertainty measures for the Level 1 annual mean control inversion (Gurney et al. 2002a). The first uncertainty measure is the mean of the individual model flux uncertainties (circles) which we designate the "within-model" uncertainty. For any region, this estimated flux uncertainty must be smaller than the prior flux uncertainty (outer bounds of the boxes). The magnitude of the decrease indicates the degree to which the final flux estimate is constrained by the CO_2 measurements. Figure 1 shows that the northern land regions and Australia are better constrained by the measurements than the remaining land regions. The Southern Ocean region is well constrained by the atmospheric measurements, in part because it is treated as a single large region. The Atlantic regions are constrained more by their prior flux uncertainties, which are relatively small due to better coverage of ocean measurements in these regions.

The second uncertainty measure is the standard deviation of the flux estimates over the ensemble of models (error bars). We call this the "between-model" uncertainty. This measure indicates the degree to which transport model differences contribute to the range of flux estimates. Large between-model uncertainties are found for northern Africa, tropical America, temperate Asia and boreal Asia (all greater than 0.5 GtC/year).

For most regions, the between-model uncertainties are of similar or smaller magnitude than the within-model uncertainties. This suggests that the choice of transport model is not the critical determinant of the inferred fluxes. Comparing the uncertainties between regions indicates where the inversion would benefit most from new observations and where model improvements are most needed. In this particular inversion, new measurements would be most useful over tropical continents and in the South America and South Atlantic regions while the focus for resolving transport differences would be the northern and tropical land regions.

Regarding the model mean flux estimates, two results deserve attention. First, consistency is found between the ocean fluxes predicted in the annual mean fluxes and those based on a global pCO_2 database (Takahashi et al. 1999), except in the Southern Ocean where the carbon uptake estimated here is roughly half that based on the pCO_2 database. This shift in uptake from south to north is required to simultaneously match large-scale concentration gradients and growth rates.

Second, we find carbon uptake over the Northern Hemisphere continents distributed relatively evenly across North America, Europe, and Asia, in contrast to the distribution found in an earlier, widely cited inverse study (Fan et al., 1998). We find a temperate North American sink approximately 60% of that found in the earlier study, a small boreal North American source rather than small uptake, and a large sink for Eurasia rather than an approximately neutral flux. Estimated uncertainties are moderate (0.4-0.7 GtC/year) indicating that regional partitioning remains difficult, but the flux differences between the two studies lie at the edge or outside the uncertainty ranges.

While transport uncertainties do not overwhelm the annual mean, model mean flux estimates, one factor appears to be responsible for a significant portion of the model spread; the "rectifier" produced by the covariance between the seasonal biospheric background flux and atmospheric transport (Keeling et al., 1989; Denning et al., 1995). The impact of the rectifier can be seen by performing the inversion without the background biospheric fluxes (Figure 1, right symbols within each box). The between-model uncertainty is reduced for almost all regions and in some regions there are substantial changes to the estimated fluxes. An

increase of 1.1 GtC/year in boreal Asia changes it from a moderate sink to a moderate source because rectification produces the strongest concentrations downwind of this region in many of the models. Sink strengths increase by 0.35 - 0.55 GtC/year for temperate North America, temperate Asia and northern Africa, to maintain the required global source.

To test the dependence of the model-mean inversion to the prior fluxes and their uncertainties, a series of sensitivity tests were performed and are listed in Table 1 (Gurney et al. 2002b).

Table 1. Brief description of the sensitivity tests.

Test 1 ("Loose Priors"): The prior flux uncertainties for both land and ocean basis function regions are increased to 2, 5, and 10 GtC yr^{-1}. These cases bring the inversion closer to those methods that do not use prior information to constrain the flux estimates.
Test 2 ("Zero Priors"): The prior basis function land fluxes are set to zero. Since many tropical regions are not well-observed, it is important to check how sensitive the flux estimates are to the inclusion of land-use change information in the prior flux estimates.
Test 3 ("No Rect"): The background biospheric exchange is set to zero. This tests the sensitivity of the flux estimates to the rectifier.
Test 4 ("Adjust Rect"): The background biosphere exchange flux uncertainty is set to ± 1 GtC yr^{-1}. This tests what rectifier magnitude the inversion estimates.
Test 5 ("Zero Ocean"): The background ocean exchange is set to zero. This tests whether the inversion is sensitive to the spatial distribution in the background ocean flux.

The results of the first test are presented in Figure 2. For most regions, the mean flux estimates (x symbols) are very insensitive to the prior information, and lie within the uncertainty range of the control inversion. Exceptions are regions with few (or no) stations: the tropical and South Atlantic (all cases), northern Africa (±5 and ±10 GtC/year cases) and southern Africa and South America (±10 GtC/year case).

Figure 3 shows results from the other four sensitivity tests. When the land prior fluxes were set to zero only the estimated tropical Asian flux changed by greater than 0.2 GtC/year. Even for this region, the new flux estimate does not lie outside the control uncertainty range, which at 0.74 GtC/year is not much smaller than its prior uncertainty of 0.87 GtC/year. This is because none of the 76 sites used in the control inversion contributes much constraint to this region. Hence, with this dataset, it is difficult to confirm or deny the prior terrestrial flux of 0.8 GtC/year.

As described above, removing the background biosphere fluxes (third set of estimates in Figure 3) has a large impact in some northern regions where rectification is pronounced; mean flux estimates change by up to 1.1 GtC yr^{-1} and between-model uncertainty is generally reduced. For example, in almost all models, Boreal Asia changes from a moderate sink to a moderate source. In Test 4, we allow the inversion to optimize the magnitude of the seasonal rectifier, which tends to produce fluxes that are mid-way between the control and the no rectifier case. There is no "consensus rectifier" scaling: the range of estimates of rectifier magnitude among the models spans the range of 0 to 1. In the final test, removing the background ocean flux had a larger impact in many of the land regions compared to oceanic regions, probably due to the generally larger prior uncertainties for land regions. However none of the flux changes is larger than the control within-model uncertainties for the appropriate region, indicating that the flux estimates are robust to this sensitivity test.

2.1.2 Individual model results. Some of the individual model estimated fluxes can be readily attributed to how they respond to the background flux fields (Figures 4 and 5)[1]. Table 2 lists the control inversion flux

[1] A 17th model (CSIRO) recently submitted simulations. We have not included results from this model in the calculation of mean results, in order to maintain consistency with the model mean calculations but have included it in presentations of individual model results.

estimates for the individual models when the land and ocean regions have been aggregated separately into the southern extratropics, tropics and northern extratropics.

Table 2. Aggregated posterior fluxes and within-model uncertainties (1σ) for individual models, control inversion. The background ocean flux has been included in the oceanic fluxes. Regional aggregation is as follows: North land (Boreal North America, Temperate North America, Europe, Boreal Asia, Temperate Asia), North ocean (North Pacific, Northern Ocean, North Atlantic), Tropical land (Northern Africa, Tropical Asia, Tropical America), Tropical ocean (West Pacific, East Pacific, Tropical Atlantic, Tropical Indian), South land (Southern Africa, Australasia, South America), South ocean (South Pacific, South Atlantic, South Indian, Southern Ocean). The mean sources do not include the CSIRO model. Units: GtC yr^{-1}

Region	North land	North Ocean	Tropical land	Tropical Ocean	South land	South Ocean	Total Land	Total Ocean
CSU	-2.5±0.6	-1.7±0.5	2.8±1.4	0.9±0.8	-0.7±1.2	-1.6±0.6	-0.5±1.3	-2.4±1.3
UCB	-2.9±0.6	-1.1±0.6	2.1±1.3	0.3±0.7	-0.4±1.1	-0.8±0.7	-1.1±1.2	-1.7±1.2
UCI	-1.4±0.7	-1.6±0.6	-0.3±1.4	0.8±0.7	0.7±1.0	-1.0±0.7	-1.1±1.2	-1.7±1.2
UCIs	-1.5±0.7	-1.1±0.6	-0.8±1.3	1.1±0.7	0.3±1.2	-0.8±0.7	-2.0±.13	-0.8±1.3
UCIb	-1.4±0.7	-1.6±0.6	-0.4±1.4	0.9±0.6	0.7±1.0	-1.0±0.7	-1.1±1.1	-1.7±1.1
JMA	-2.0±0.7	-0.7±0.6	0.9±1.5	-0.0±0.7	0.1±1.2	-1.1±0.8	-1.0±1.3	-1.8±1.3
M:CCM3	-2.5±0.6	-0.7±0.5	0.7±1.3	0.6±0.7	-0.3±1.1	-0.6±0.6	-2.1±1.2	-0.7±1.2
M:NCEP	-3.6±0.5	-0.0±0.4	2.2±1.2	0.6±0.7	-2.0±1.0	0.1±0.6	-3.4±1.1	0.6±1.1
M:MACCM2	-3.4±0.6	-0.3±0.5	1.8±1.4	0.8±0.8	-0.3±1.2	-1.4±0.7	-1.9±1.2	-0.9±1.2
NIES	-3.2±0.6	-0.5±0.4	2.2±1.3	-0.3±0.6	-0.1±1.1	-0.8±0.7	-1.2±1.0	-1.6±1.0
NIRE	-2.5±0.6	-2.1±0.4	1.2±1.3	0.5±0.5	0.4±1.1	-0.4±0.6	-0.8±0.9	-2.0±0.9
RPN	-2.0±0.6	-1.3±0.4	1.0±1.0	-0.4±0.7	-0.2±0.9	0.1±0.6	-1.2±1.1	-1.6±1.1
SKYHI	-3.2±0.6	-0.9±0.3	2.9±1.3	-0.2±0.6	-0.5±1.1	-1.0±0.6	-0.7±1.0	-2.1±1.0
TM2	-0.8±0.6	-1.6±0.5	-0.2±1.5	-0.0±0.5	0.6±1.2	-0.9±0.7	-0.3±1.2	-2.5±1.2
TM3	-3.1±0.5	0.1±0.4	1.4±1.2	0.5±0.6	-0.5±1.1	-1.2±0.7	-2.2±1.1	-0.6±1.1
GCTM	-1.2±0.5	-1.6±0.4	0.8±1.4	0.2±0.6	-0.4±1.2	-0.5±0.6	-0.9±1.0	-1.9±1.0
CSIRO	-2.7±0.6	-0.1±0.4	1.3±1.3	0.5±0.8	-1.3±1.1	-0.5±0.7	-2.7±1.2	-0.1±1.2
Mean	**-2.3±0.6**	**-1.1±0.5**	**1.1±1.3**	**0.4±0.7**	**-0.2±1.1**	**-0.8±0.7**	**-1.3±1.1**	**-1.5±1.1**

Figure 6 shows similar information, plotted as *differences from the mean flux* for each region, along with flux differences for the 'No Rect' (sensitivity test 3) and 'Zero Ocean' (sensitivity test 5) sensitivity tests. The tighter ocean constraints of the inversion setup and the greater variability in model response to the terrestrial background fluxes explain the greater model spread in the estimates for land versus ocean regions. Removal of the background biospheric exchange considerably reduces the model spread over land. Furthermore, the tropical land exchange is inversely related to the northern land uptake, highlighting the influence of the limited observational constraint in the tropical regions and the required compliance with the overall meridional gradient in the CO_2 observations. The influence of the rectifier emphasizes the need to observe and understand this phenomenon. Because incorrect spatial and temporal structure in this background flux cannot be adjusted by the inversion procedure, errors in the specification of the background flux will be aliased into errors in the regional flux estimates. Allowing the inversion to adjust the temporal and spatial structure of the terrestrial fluxes will be reported in the seasonal and interannual cases discussed below.

The last conclusion that can be drawn from the aggregated flux estimates is the relationship between the Southern Ocean uptake and interhemispheric transport; models with small background flux interhemispheric differences (see Figure 5), and hence more vigorous interhemispheric transport, tend to estimate the greatest reduction in uptake when compared to the background ocean flux for this region. Models with larger background flux interhemispheric differences tend to have a more moderate uptake reduction. Like many of the other broad relationships between the background fluxes and the estimated model fluxes, this relationship is not universal to all the models and some exceptions remain.

Examination of the 22 regional flux estimates (Table 3) across the models further indicates some relationships to the background flux responses though generalization is much more challenging. For example, models with a strong response to the background ocean flux estimate the weakest uptake in both the Southern Ocean and northern ocean regions. Models with large west to east background to predicted CO_2 concentration gradients across North America and Europe, are among the models with the greatest uptake in these regions. However, models with weak gradients are not necessarily those with little uptake in these regions. Furthermore, the estimated fluxes in northern extratropical Asia appear to have a limited relationship to the distribution of background flux response. Asia, however, is where the largest changes occur in individual model flux estimates when the background biosphere exchange is removed from the inversion. Most models exhibit large changes in their estimated flux when this change is made, often changing from a sink to a source.

In many instances, the model-to-model differences appear to reflect particular individual model responses at stations. Some of this is due to the coincidence of strong concentration gradients and station locations while some may be due to local transport differences at the surface such as convective transport or the construction of the planetary boundary layer (PBL). In the case of the UCI model and its two variants, the version that incorporates a resolved stratosphere tends to respond to the background fluxes and estimate posterior fluxes with greater differences than those between the base UCI model and the variant with a planetary boundary layer.

2.1.3. Sensitivity to data choices. Four categories of data sensitivity have been examined in the annual mean case: the network station list, the time period, the model output sampling methodology, and the construction of data uncertainty. The annual mean control case made particular choices regarding each of these categories. They are as follows:

1. A station was included in the control case network if it exhibited more than 70% measured versus interpolated data.
2. The time period was chosen as 1992 to 1996.
3. A method was specified in the experimental protocol that guided modelers in sampling their forward simulations in a fashion similar to that employed in the Globalview network.
4. The data uncertainty in the control inversion employed a spatially explicit uncertainty based on the GlobalView RSD values but scaled to achieve a normalized X^2 value close to 1.0 (see Gurney et al. 2002a for further elaboration).

The results for running the inversion using different networks is shown in Figure 7. Overall, most flux estimates lie within the uncertainty range of the control case, which suggests that most regions are not too sensitive to the network choice. Figure 8 summarizes the inversion sensitivity to different observational time periods. Most regions show limited sensitivity to the time period considered and closer examination of the results (see Law et al., 2002b) indicate that the differences that emerge are due to interannual differences in the CO_2 observations themselves rather than differences in the atmospheric growth rate or the underlying fossil emissions. Two regions, temperate North America and Tropical Indian ocean, show changes that exceed 0.5 Gt C/year in the sensitivity tests. For the latter, the strongly result is dependent upon two stations, Seychelles and Darwin, which exhibit anomalous concentration values. For temperate North America, the greater uptake in the 1989 – 1991 period appears to be reflective of consistent changes in the observational data in and around this region.

Figure 9 shows the result of employing different sampling strategies to the model output which includes both more and less selection than considered in the control inversion. Once again, the results do not show great sensitivity to this category of the inversion but does exhibit some individual cases worth noting. For example, Temperate North America change by over 1.0 Gt C/year when less selection is employed. This is due almost entirely to the response at Key Biscayne which in the control inversion is sampled off-shore. Moving the sampling on-shore increases the fossil signal substantially thereby requiring a greater sink in order to match the observational constraint.

The last sensitivity test is shown in Figures 10 and 11; altering the "data uncertainty" assigned to the observational CO_2 concentrations. The clearest feature from Figure 10 is the change in relative magnitude of the within-model and between-model uncertainties. As data uncertainty is increased, the within-model uncertainty increases and the between-model uncertainty decreases and vice-versa. When data uncertainty is decreased the inversion is forced to fit the data more closely. This accentuates model transport differences and hence large between-model uncertainty results. The results from figure 11 indicate the impact data uncertainty configuration can have on the inversion. The last two cases show the largest changes and reflect data uncertainty choices that most of the inversion community, at this point in time, would consider ill-advised.

2.2. Seasonal carbon sources and sinks

Figure 12 shows the estimated seasonal fluxes, prior fluxes, and uncertainties for the ocean and land regions combined into north, tropical, and south aggregates. The estimated fluxes have been added to the neutral biosphere prior flux for the land and the Takahashi ΔpCO_2-based prior fluxes for the ocean. The flux uncertainties are large in all regions except the northern land where a number of months depart significantly from the prior flux. In the northern hemisphere land region, the results suggest less emission during March and April and greater uptake during May, June, and July relative to the prior flux. Also shown are the model mean estimated fluxes when the inversion is run without the neutral biosphere prior flux on land. There is little differences between the two cases (with neutral biosphere and without) indicating that for these aggregated regions, the estimated fluxes are primarily driven by the observational data and the atmospheric growth rate constraints.

Disaggregation of the northern hemisphere region is shown in Figure 13. In temperate North America, the estimated fluxes are positioned below the prior flux values in all times of the year though the uncertainties are large. The Boreal North America fluxes appear to be consistent with the prior fluxes except in June where the estimated flux exhibits less uptake than suggested by the prior. A similar feature appears in the estimated seasonal fluxes for the Boreal Asia region in addition to less emissions in Spring relative to the prior flux. Temperate Asia, on the other hand exhibits much greater uptake in the month of June relative to the prior. In Europe this occurs in months June through September. As with the aggregated results, the removal of the neutral biosphere prior flux does not measureably alter the estimated fluxes for any of the regions. The timing of the maximum uptake shifts by one month in the temperate Asian region but the adjustment is well within the uncertainty for either month.

The ability of the participating models to correctly capture the amplitude of the CO_2 seasonal cycle at the observation stations may provide a way of comparing the strength of a given models rectifier. We represent the strength of the rectifier by computing the annual mean interhemispheric surface CO_2 concentration from the forward simulation of the neutral biospheric flux. Models with strong rectification produce large interhemispheric gradients in this tracer and vice versa. The ability of a model to capture the seasonal cycle is computed by first determining the maximum predicted peak to peak (ptp) concentration at each of the stations in the inversion. This is then compared to the observational value the root mean square error in the seasonal amplitude is computed over all the stations north of 35 N latitude. Figure 14 shows the relationship between these two indices. Two groupings result: models with large ptp mismatches tend to have weak rectifiers while models exhibiting small ptp mismatches tend to have stronger rectification. While the relationship has considerable scatter, the results suggest that models showing strong rectification do a better job at capturing the seasonal cycle at the northern hemisphere stations.

3. Conclusions

The TransCom 3 experiment was structured such that the forward simulations across all the participating models would begin with the level 1 simulations and sequentially finish with Level 3. Though analysis continues on the recently-received seasonal and interannual aspects of the experiment, a number of conclusions can be drawn from the annual mean and preliminary seasonal inversion results.

1. **The annual mean/model mean estimated flux finds a northern hemisphere land carbon sink evenly distributed across longitude.**

2. **For the annual mean inversion, the uncertainty resulting from different simulated transport is roughly equivalent to that due to the uncertainty in CO_2 distributions resulting from sparse measurements, variable concentration, and representativeness issues. Estimated fluxes in all regions would benefit from more observations in the tropical regions. Uncertainty in transport characteristics (across models) dominates flux uncertainty over some well-observed regions, particularly in the northern midlatitudes.**

3. **All the models consistently agree on weaker Southern Ocean carbon uptake in the annual mean relative to fluxes based on ΔpCO2 measurements. This feature was insensitive to model transport, and reflects an abundance of year-round atmospheric measurements on the Antarctic coast.**

4. **In most regions, the model mean/annual mean flux estimates are quite insensitive to details of the inversion set-up such as the prior flux estimates and prior flux uncertainties. The exception is in the poorly-observed tropical land regions, where data constraint is weak.**

5. **The model mean/annual mean flux estimates are relatively insensitive to data uncertainty choices, though certain observational stations can have an influence on particular regions.**

6. **Individual model results for the annual mean inversion show sensitivity to the transport of the presubtracted tracers. This is particularly true for the regionally aggregated results. When examined at the full regional resolution, generalization about response to background tracers is harder to come by. In some cases, results are idiosyncratic and result from sensitivities to particular stations.**

7. **The model mean seasonal inversion flux estimates for the northern hemisphere land feature stronger uptake during the growing season and reduced net emission in other seasons, as compared to the neutral biospheric prior flux. This feature appears in all the regions at full resolution except for Boreal North America.**

8. **The ability of the individual models to capture the maximum peak to peak concentration at the observational stations used in the seasonal control inversion tends to scale with the strength of the seasonal rectifier. Those models with stronger rectification tend to capture this seasonality better than those with weak rectification.**

Further results and discussion on these conclusions can be found in recently published and submitted papers (Gurney et al 2002a; Gurney et al., 2002b; Law et al., 2002b)

4. The future

Currently, the primary focus of the TransCom 3 experiment is on the interpretation of the seasonal inversion results with a publication to be submitted in the coming months. Emphasis also continues on the inversion of the interannual CO_2 data with results to be presented at the American Geophysical Union meeting in San Francisco, December 2002. As can be seen from the publication/presentation list in the Appendix, a variety of other sensitivity and original research work has utilized the TransCom experimental output. This is expected to continue for some time, particularly in light of the upcoming public availability of the TransCom 3 model output. This voluminous simulation database will serve as a source of original work far into the future. Maintaining open and easy access to this database is a priority and will be maintained at Colorado State University with support from the National Oceanic and Atmospheric Administration.

At the last TransCom 3 workshop in Colorado (February 2002), there was general agreement among the participants that further coordination and meeting would prove beneficial to the analysis of the TransCom 3 results and to the benefit of the general CO_2 inverse community. An additional workshop is being planned for 2003 at the Max Planck Institut fur Biogeochemistry in Jena, Germany to be hosted by the Martin Heimann group.

5. References

Enting, I. G., C. M. Trudinger, and R. J. Francey, A synthesis inversion of the concentration and $\delta^{13}C$ of atmospheric CO_2, *Tellus* , **47B** , 35-52, 1995.

Fan, S. et al. 1998. A large terrestrial carbon sink in North America implied by atmospheric and oceanic CO_2 data and models. *Science*, **282**, 442-446.

Gurney, K., Law, R., Rayner, P., and Denning, A.S. 2000. TransCom 3 Experimental Protocol, Department of Atmospheric Science, Colorado State University, USA, Paper No. 707.

Gurney, K.R., R.M. Law, A.S Denning, P.J. Rayner, D. Baker, P. Bousquet, L. Bruhwiler, Y.H. Chen, P. Ciais, S. Fan, I.Y. Fung, M. Gloor, M. Heimann, K. Higuchi, J. John, T. Maki, S. Maksyutov, K. Masarie, P. Peylin, M. Prather, B.C. Pak, J. Randerson, J. Sarmiento, S. Taguchi, T. Takahashi, C.W. Yuen, "Towards robust regional estimates of CO_2 sources and sinks using atmospheric transport models," *Nature,* **415**, pp. 626-630, February 7, 2002.

Gurney K.R., et al., "Transcom 3 Inversion Intercomparison: 1. Annual mean control results and sensitivity to transport and prior flux information," submitted to *Tellus*, 2002.

Law, R.M., P.J. Rayner, L.P. Steele, I.G. Enting Using high temporal frequency data for CO_2 inversions. *Global Biogeochemical Cycles*, in press, 2002.

Law, R., Y.H. Chen, K.R. Gurney, P. Rayner, A.S. Denning, and TransCom 3 modelers, "TransCom3 CO_2 inversion intercomparison: 2. Sensitivity of annual mean results to data choices," submitted to *Tellus*, 2002.

Rayner, P. J., Enting, I.G., Francey, R.J. and Langenfelds, R.L. 1999. Reconstructing the recent carbon cycle from atmospheric CO_2, $\delta^{13}C$ and O_2/N_2 observations. *Tellus*, **51B**, 213-232.

Takahashi, T. *et al.* 1999. Net sea-air CO_2 flux over the global oceans: An improved estimate based on the sea-air pCO_2 difference. Proceedings of the 2nd CO_2 in Oceans Symposium, Tsukuba, Japan.

Tarantola, A. 1987. *Inverse Problem Theory: Methods for Data Fitting and Parameter Estimation*, Elsevier, Amsterdam.

Appendix A: TransCom 3 related papers and presentations

Peer-reviewed literature:

Engelen, R.J., A. Scott Denning, K.R. Gurney, and TransCom 3 modelers, "On Error Estimation in Atmospheric CO_2 Inversions" accepted to *Journal of Geophysical Research*, 2002.

Gurney, K.R., R.M. Law, A.S Denning, P.J. Rayner, D. Baker, P. Bousquet, L. Bruhwiler, Y.H. Chen, P. Ciais, S. Fan, I.Y. Fung, M. Gloor, M. Heimann, K. Higuchi, J. John, T. Maki, S. Maksyutov, K. Masarie, P. Peylin, M. Prather, B.C. Pak, J. Randerson, J. Sarmiento, S. Taguchi, T. Takahashi, C.W. Yuen, "Towards robust regional estimates of CO_2 sources and sinks using atmospheric transport models," *Nature,* **415**, pp. 626-630, February 7, 2002.

Gurney K.R., et al., "Transcom 3 Inversion Intercomparison: 1. Annual mean control results and sensitivity to transport and prior flux information," submitted to *Tellus*, 2002.

Law, R.M., P.J. Rayner, L.P. Steele, I.G. Enting Using high temporal frequency data for CO_2 inversions. *Global Biogeochemical Cycles*, in press, 2002.

Law, R., Y.H. Chen, K.R. Gurney, P. Rayner, A.S. Denning, and TransCom 3 modelers, "TransCom3 CO_2 inversion intercomparison: 2. Sensitivity of annual mean results to data choices," submitted to *Tellus*, 2002.

Maksytuov, S., T. Machida, H. Mukai, P. Patra, T. Nakazawa, G. Inoue, and TransCom 3 modelers, "Effect of recent observations on Asian CO_2 flux estimates with transport model inversions," submitted to *Tellus*, 2002.

Patra, P.K., S. Maksyutov, and TransCom 3 modelers, "Optimal network design for improved CO_2 source inversion," submitted to *Tellus*, 2002.

Pak, B.C., and M.J. Prather, "CO_2 source inversions using satellite observations of the upper troposphere," *Geophys. Res. Lett.*, **28**, 4571-4574, 2001.

Roy, T. P. J. Rayner, R. Matear and R. Francey, "Southern hemisphere ocean CO_2 uptake: Reconciling atmospheric and oceanic estimates," *Tellus*, 2002, in press.

Rayner, P.J. and R. M. Law and D. M. O'Brien and T. M. Butler and A. C. Dilley, "Global observations of the carbon budget: III. Initial assessment of the impact of satellite orbit, scan geometry and cloud on measuring CO_2 from space," *J. Geophys. Res.,* 2002, in press.

Presentations:

"TransCom 3: Carbon Inversion Intercomparison," Workshop on Inverse Methods in Global Biogeochemical Cycles, K.R. Gurney, P. Rayner, R. Law, and S. Denning, Heraklion, Greece, March 16, 1998.

"Atmospheric Carbon cycle Inversion Intercomparison (TransCom 3)," K.R. Gurney, P. Rayner, R. Law, and S. Denning, 1998, presented at Fall 1998 AGU Meeting, San Francisco.

"TransCom 3: Atmospheric Carbon Budget Inversion Intercomparison," K.R. Gurney, P. Rayner, R. Law, and S. Denning, International Union of Geodesy and Geophysics, Birmingham, UK, July 21, 1999

"Atmospheric Carbon Budget Inversion Intercomparison: Preliminary Results," K.R. Gurney, P. Rayner, R. Law, and S. Denning, presented at Spring meeting of the American Geophysical Union, May 28 – June 4, 2000. Washington DC.

"Robust regional estimates of annual mean CO_2 sources and sinks," K.R Gurney, R. Law, P.Rayner, A.S. Denning and TransCom modelers, poster presentation, Challenges of a Changing Earth, Amsterdam, June 2001.

"Towards more robust estimates of CO2 fluxes: control results from the TransCom 3 inversion intercomparison," K.R Gurney, R. Law, P.Rayner, A.S. Denning and TransCom 3 modelers, presentation to NOAA PI meeting, Princeton, NJ, August 2001.

"Uncertainty in the TransCom 3 Control Inversion," K.R Gurney, R. Law, P.Rayner, A.S. Denning and TransCom 3 modelers, presentation to carbon Modeling Consortium meeting, Princeton, NJ, August 2001.

"The TransCom 3 Experiment: Key Results from an Atmospheric Carbon Cycle Inversion

Intercomparison," K.R. Gurney, Rachel Law, Peter Rayner, Scott Denning and TransCom 3 modelers, talk presented at the 6th International Carbon Dioxide Conference, Sendai, Japan, October 1–5, 2001.

"Sensitivity of Japan Meterological Agency Carbon Dioxide Transport Model to Carbon Dioxide Monitoring Network," T. Maki, T. Koide, T. Sasaki and TransCom 3 modelers, poster presented at the 6th International Carbon Dioxide Conference, Sendai, Japan, October 1–5, 2001.

"Using transport model bias to assess the reliability of inversion results," A.S. Jacobson, J.L. Sarmiento, S. Fan, N. Gruber, and TransCom 3 modelers, poster presented at the 6th International Carbon Dioxide Conference, Sendai, Japan, October 1–5, 2001.

"Optimal Network Design for CO_2 Observations Maximizing the Inversion Performance," P.K.Patra, S. Maksyutov and TransCom 3 modelers, poster presented at the 6th International Carbon Dioxide Conference, Sendai, Japan, October 1–5, 2001.

"Overview of the Atmospheric CO_2 Inversion Intercomparison Project (TransCom3)," Denning, A.S., K.R. Gurney, R.M. Law, P.J. Rayner, and TransCom 3 Modelers, presented at Sixth International Carbon Dioxide Conference, October 1-5, 2001, Sendai, Japan.

"Potential Constraints on the Global Carbon Budget Using Satellie Retrievals of Atmospheric CO_2," A.S. Denning, K.R. Gurney, R. Engelen, G. Stephens, D.O'Brien, P.J. Rayner and TransCom 3 modelers, poster presented at the 6th International Carbon Dioxide Conference, Sendai, Japan, October 1–5, 2001.

"Asian CO_2 Fluxes Estimated Using Recent Observations and Transport Model Inversions," S. Maksyutov, T. Machida, T. Nakazawa, G. Inoue, H. Mukai, P.K. Patra and TransCom 3 modelers, talk presented at the 6th International Carbon Dioxide Conference, Sendai, Japan, October 1–5, 2001.

"Using Airborne, Continental and Climatological Data to Evaluate Global Atmospheric CO_2 Inverse Models," B.B. Stephens, L. Bruhwiler, P.P. Tans, K.R. Gurney and TransCom 3 modelers, poster presented at the 6th International Carbon Dioxide Conference, Sendai, Japan, October 1–5, 2001.

"Towards robust regional estimates of CO_2 sources and sinks using atmospheric transport models," CSU departmental seminar, Kevin Robert Gurney and the TransCom 3 modelers, March 21, 2002

"Taking Apart the Global Carbon Cycle: Where is the Missing Sink?," Kevin Robert Gurney and TransCom 3 modelers, presented at University seminar, University of California, Santa Barbara, CA, May 2002.

"TransCom3: Using multiple transport models to give more robust estimates of CO_2 sources and sinks," Law, R.M., K.R. Gurney, P.J. Rayner, A.S. Denning and Transcom3 modelers, Australian Meteorological and Oceanographic Society, 9th National Conference, 18-20 Feb 2002.

"Bias and noise in inversions: how are the inversion results sensitive to the data and models used to constrain them," Law, R.M., Carbon Data-Model Assimilation (C-DAS) summer institute, NCAR, May 20-31, 2002.

"Sensitivity of Japan Meteorological Agency Carbon Dioxide Transport Model to Carbon Dioxide Monitoring Network," Maki, T. et al., Extended abstracts 6th International CO_2 Conference, Sendai, Japan, 2001.

"Optimum CO_2 Monitoring Network Design Using JMA-CDTM and Inversion Method," Maki, T. et al., Symposium on Atmospheric Composition Change, Yokohama, Japan, 2001.

"The sensitivity of prior flux and data uncertainties to the optimum CO_2 monitoring network extension," Maki, T. et al., TransCom 3 workshop, Fort Collins, USA, 2002.

Appendix B: TransCom 3 modelers

Kevin Robert Gurney
Department of Atmospheric Science, Colorado State University,
Fort Collins, CO, 80523

Rachel M. Law
CSIRO Atmospheric Research, PMB 1, Aspendale, Victoria 3195,
Australia

A. Scott Denning
Department of Atmospheric Science, Colorado State University,
Fort Collins, CO, 80523

Peter J. Rayner
CSIRO Atmospheric Research, PMB 1, Aspendale, Victoria 3195,
Australia

David Baker
National Center for Atmospheric Research (NCAR), Boulder, CO 80303

Philippe Bousquet
Laboratoire des Sciences du Climat et de l'Environment (LSCE),
F-91198 Gif-sur-Yvette Cedex, France

Lori Bruhwiler
National Oceanic and Atmospheric Administration (NOAA),
Climate Monitoring and Diagnostics Laboratory, 326 Broadway R/CG1,
Boulder, CO 80303

Yu-Han Chen
Department of Earth, Atmospheric, and Planetary Science,
Massachussetts Institute of Technology (MIT), Cambridge, MA 02141

Philippe Ciais
Laboratoire des Sciences du Climat et de l'Environment (LSCE),
F-91198 Gif-sur-Yvette Cedex, France

Songmiao Fan
AOS Program, Princeton University, Sayre Hall,
Forrestal Campus P.O. Box CN710 Princeton, NJ 08544-0710

Inez Fung
Center for Atmospheric Sciences, McCone Hall, University of California,
Berkeley, Berkeley, CA 94720-4767

Manuel Gloor
Max-Planck_Institute fur Biogeochemie, D-07701 Jena, Germany

Martin Heimann
Max-Planck_Institute fur Biogeochemie, D-07701 Jena, Germany

Kaz Higuchi
Meteorological Service of Canada, Environment Canada, Toronto,

Ontario M3H 5T4 Canada

Jasmin John
Center for Atmospheric Sciences, McCone Hall, University of California,
Berkeley, Berkeley, CA 94720-4767

Takashi Maki
Quality Assurance Section, Atmospheric Environment Division,
Observations Department, Japan Meteorological Agency 1-3-4 Otemachi,
Chiyoda-ku, Tokyo 100-8122 Japan

Shamil Maksyutov
Institute for Global Change Research,
Frontier Research System for Global Change, Yokohama, 236-0001 Japan

Philippe Peylin
Laboratoire des Sciences du Climat et de l'Environment (LSCE),
F-91198 Gif-sur-Yvette Cedex, France

Michael Prather
Earth System Science, University of California, Irvine, CA 92697-3100

Bernard C. Pak
Earth System Science, University of California, Irvine, CA 92697-3100

Jorge Sarmiento
AOS Program, Princeton University, Sayre Hall,
Forrestal Campus P.O. Box CN710 Princeton, NJ 08544-0710

Shoichi Taguchi
National Institute of Advanced Industrial Science and Technology,
16-1 Onogawa Tsukuba, Ibaraki 305-8569 Japan

Taro Takahashi
Lamont-Doherty Earth Observatory of Columbia University, Palisades, NY

Chiu-Wai Yuen
Meteorological Service of Canada, Environment Canada, Toronto,
Ontario M3H 5T4 Canada

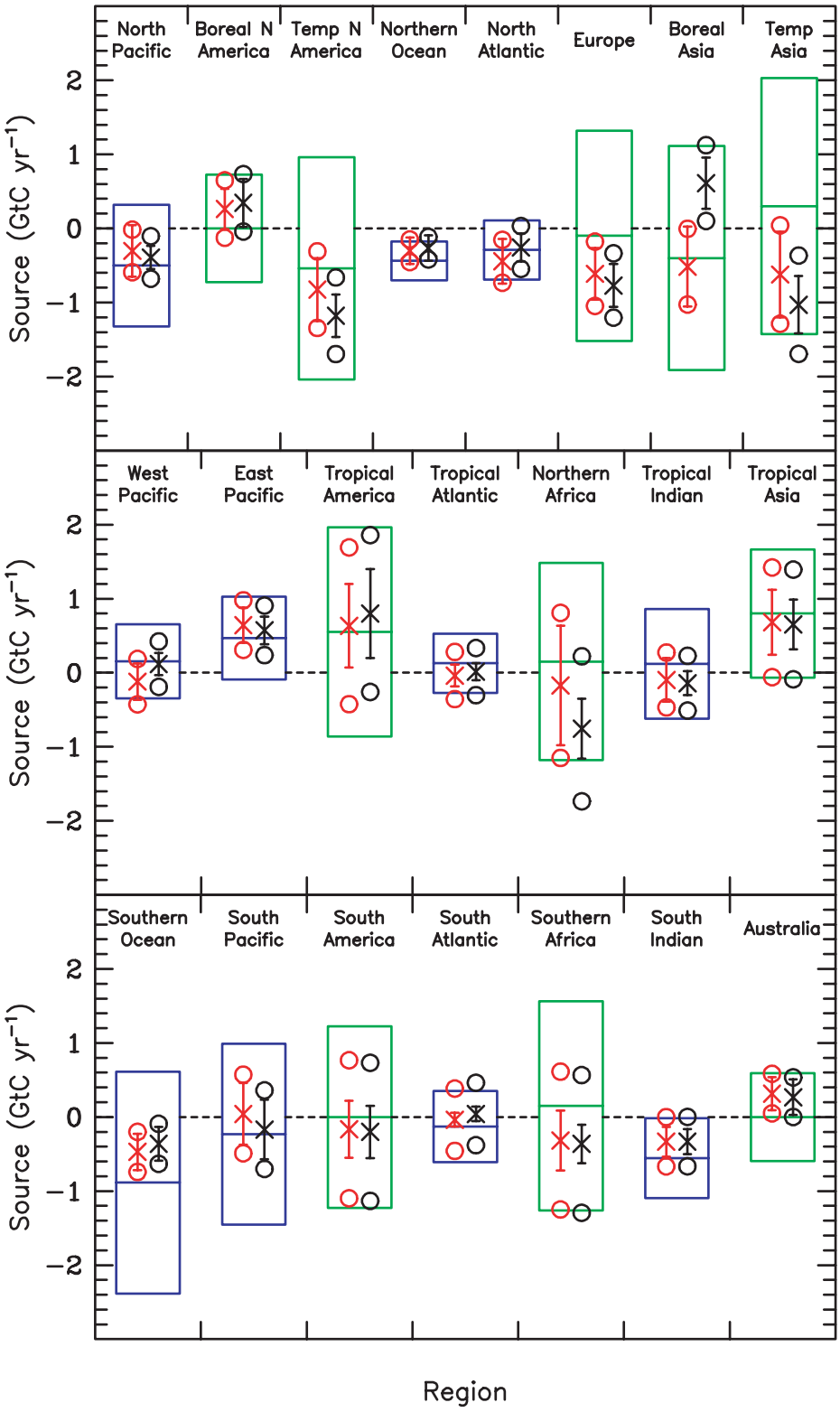

Figure 1: Mean estimated sources and uncertainties for two inversions. Red symbols in each box are for the control inversion, black symbols are for an inversion without the background seasonal biosphere flux. Mean estimated fluxes are shown by the 'X' and include all background fluxes except fossil fuel. Positive values indicate a source to the atmosphere. The prior flux estimates and their uncertainties are indicated by the boxes (green for land, blue for ocean); the central horizontal bar indicates the prior flux estimate and the top and bottom of the box give the prior flux uncertainty range. The mean estimated uncertainty across all models (the "within-model" uncertainty) is indicated by the circles. The standard deviation of the models' estimated fluxes (the "between-model" uncertainty) is indicated by the "error bars". Regions are shown in their approximate north-south and east-west relationship.

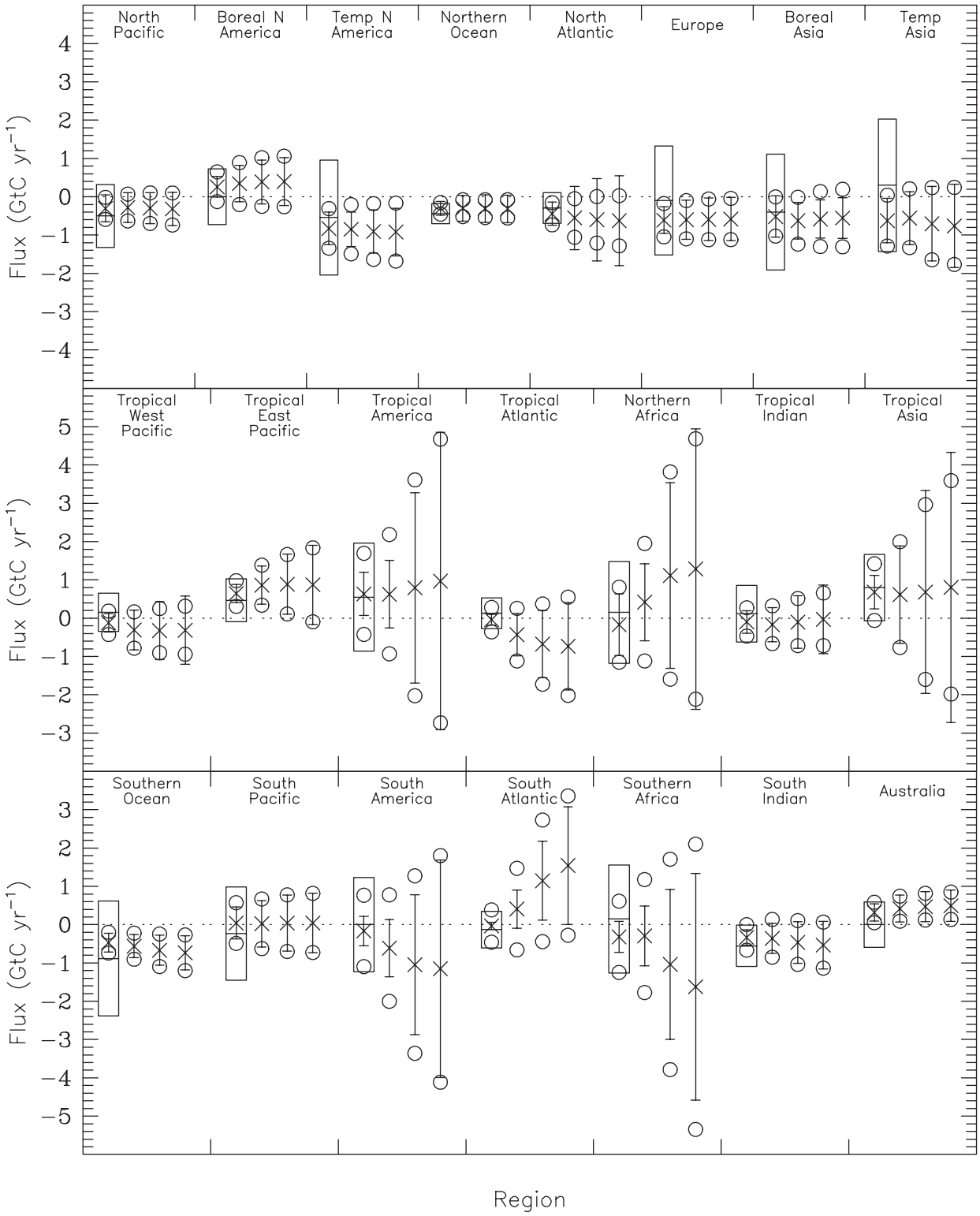

Figure 2. Results of 'Loose Priors' case (sensitivity test 1). The control inversion is denoted by the leftmost set of symbols (X - posterior flux estimate {includes background ocean exchange}; circles - within-model flux uncertainty; whiskers - between-model flux uncertainty; outer box - prior flux uncertainty). The ±2 GtCyr^{-1}, ±5 GtCyr^{-1} and ±10 GtCyr^{-1} prior uncertainty cases are denoted progressively to the right of the control inversion. All uncertainties represent 1σ. Mean does not include CSIRO.

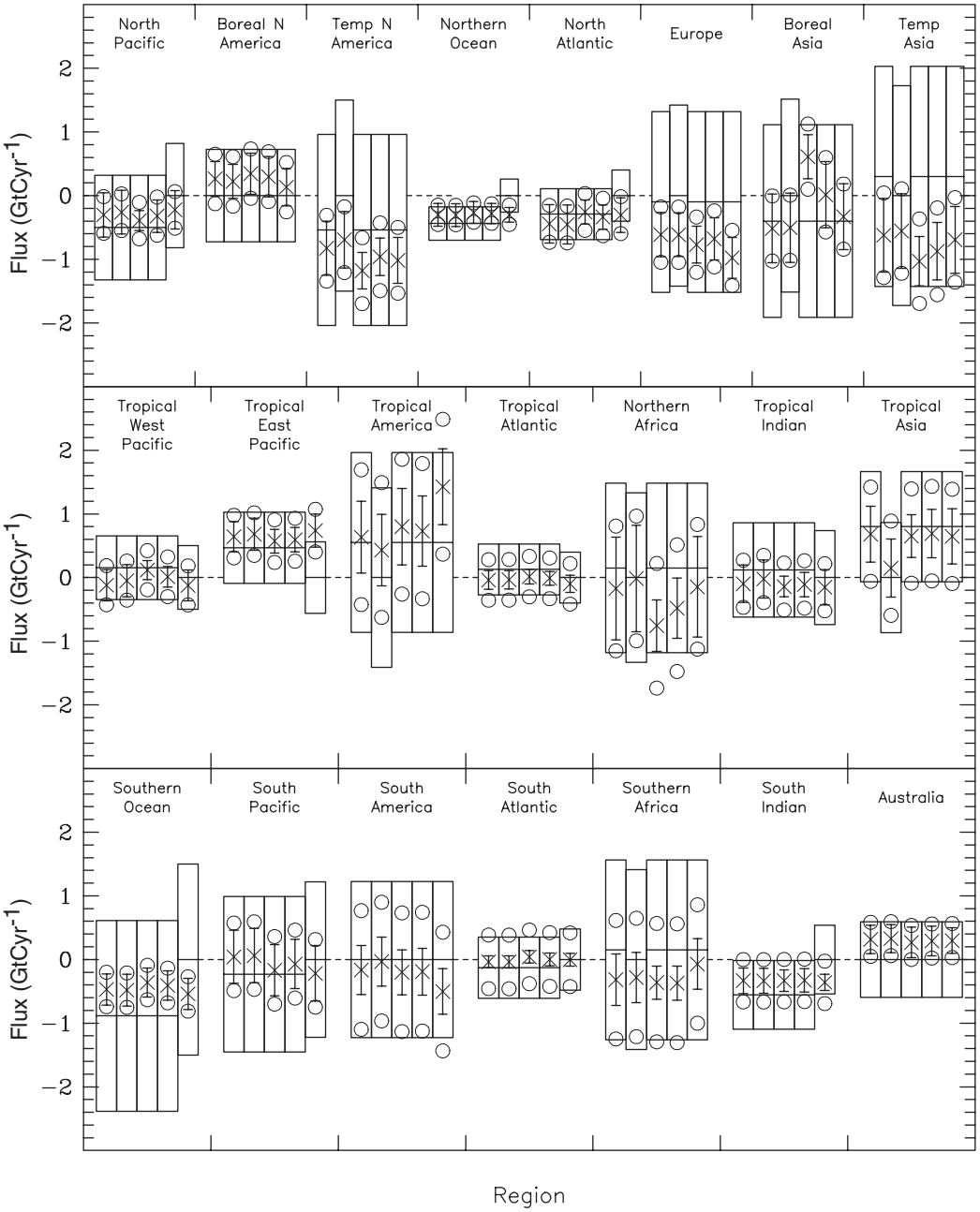

Figure 3. Results of sensitivity tests 2 through 5. The control inversion is denoted by the leftmost set of symbols (as in Fig. 2). The 'Zero Priors' case (sensitivity test 2), 'No Rect' case (sensitivity test 3), 'Adjust Rect' case (sensitivity test 4), and 'Zero Ocean' (sensitivity test 5) are denoted progressively to the right. Mean does not include CSIRO.

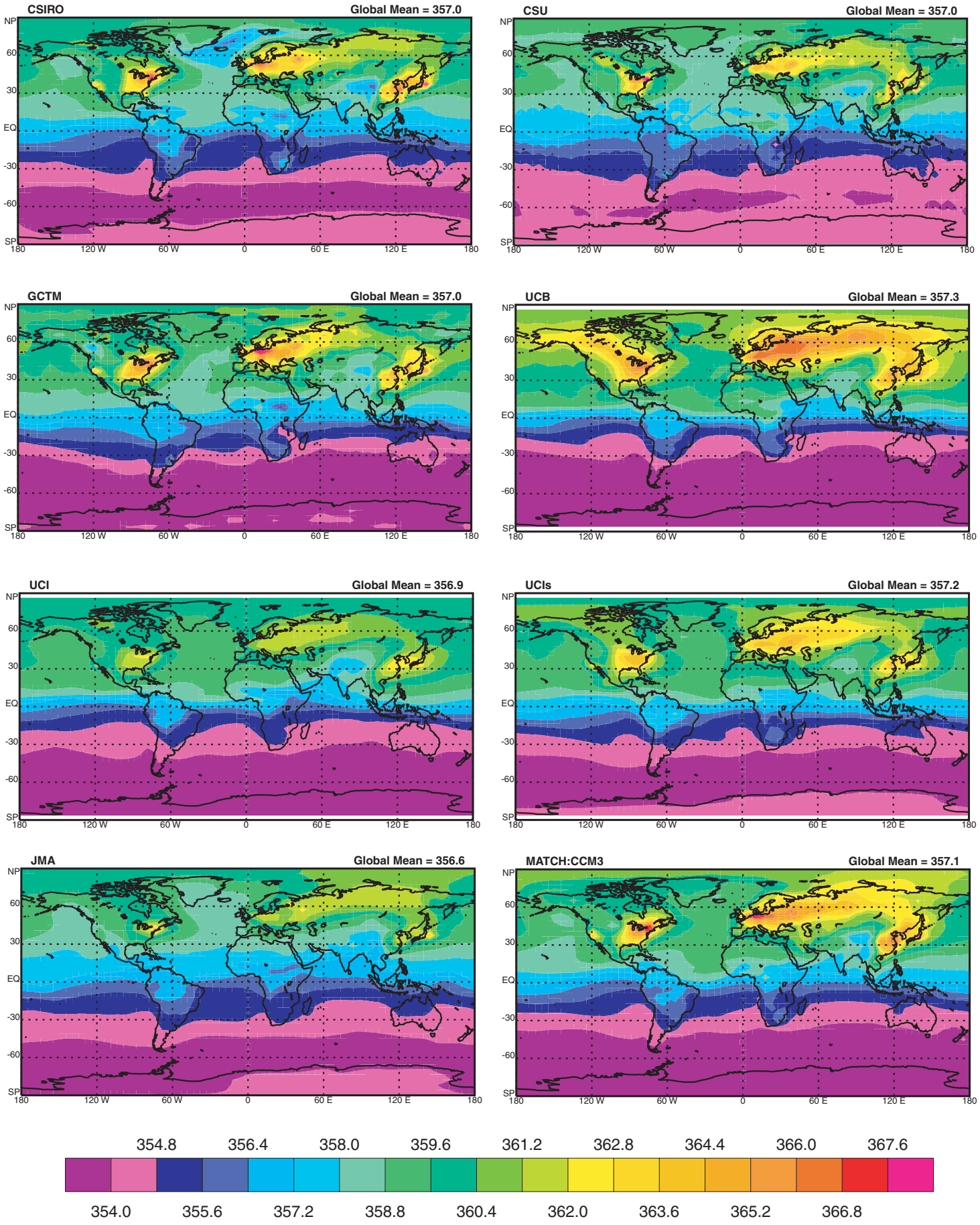

Figure 4. Annual mean surface CO_2 concentration (ppm) resulting from the combined (relative to a background concentration of 350 ppm) background fluxes for each of the models. The UCIb model variant is not shown since its surface distribution is very similar to the UCI standard version.

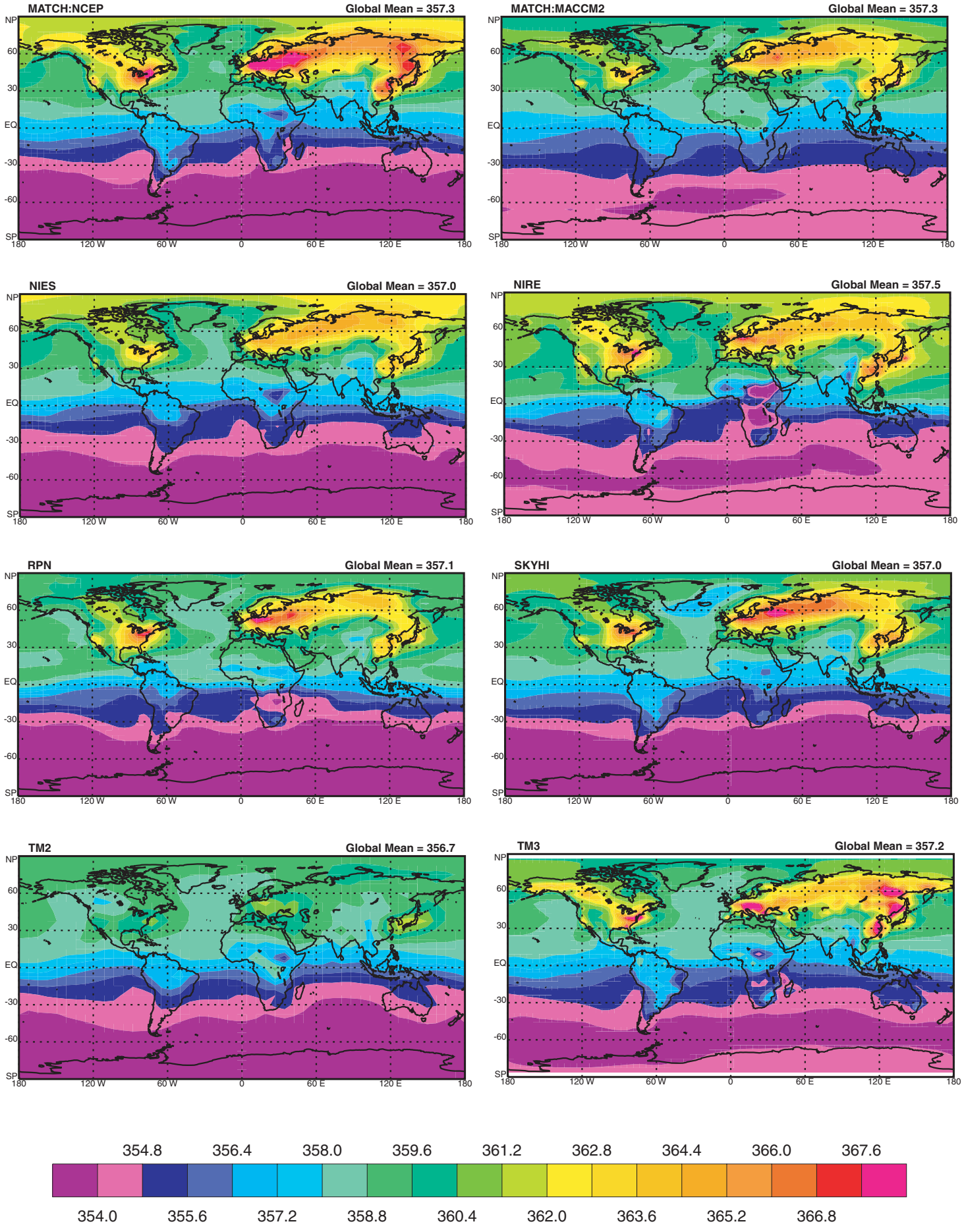

Figure 4. Continued

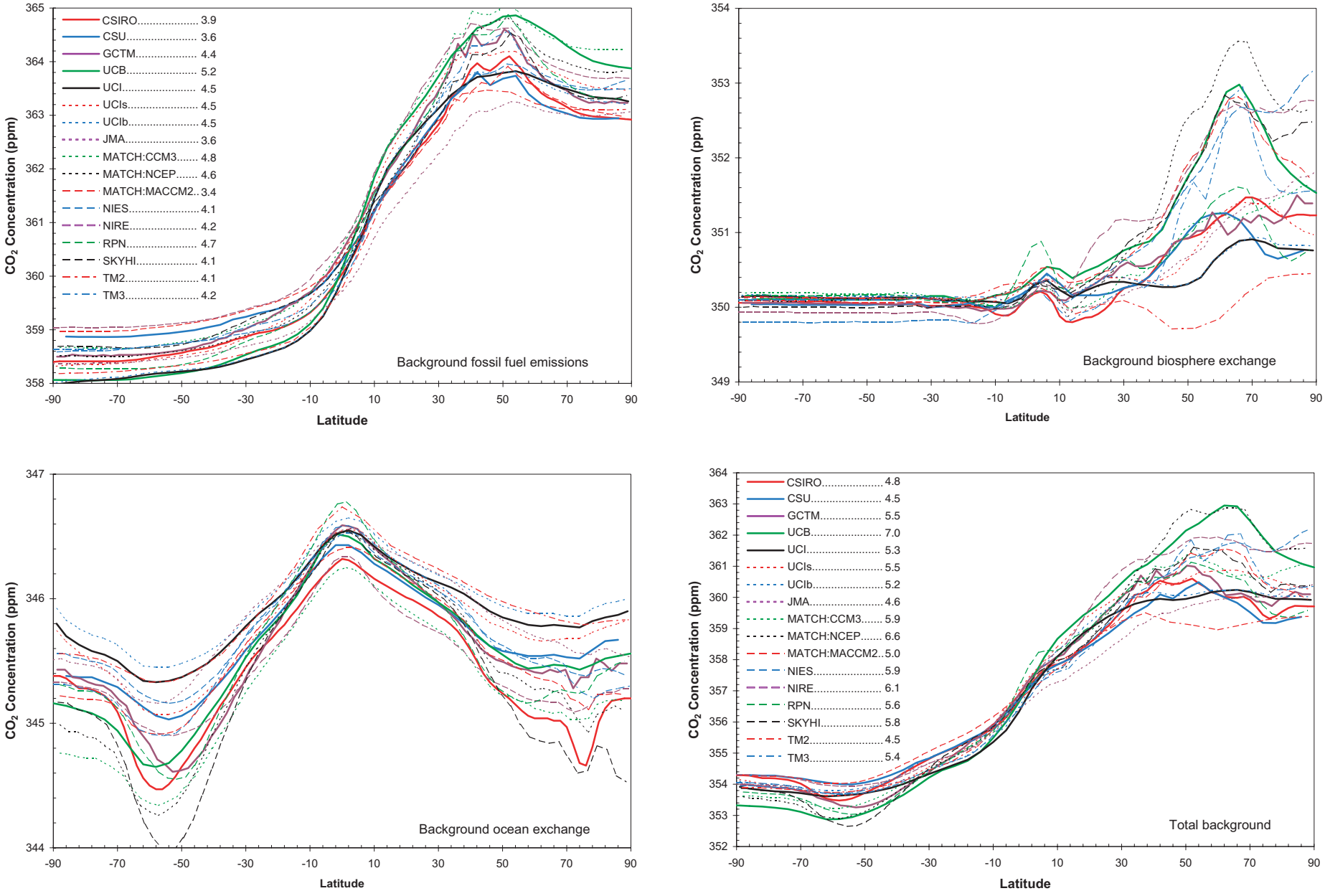

Figure 5. Annual mean, zonal mean surface CO_2 concentration (ppm) resulting from the individual and combined (relative to a background concentration of 350 ppm) background fluxes for each of the models. The interhemispheric difference (in ppm) for the background fossil and combined background CO_2 is listed in the key for each model. Note that the scale is different in each of the plots.

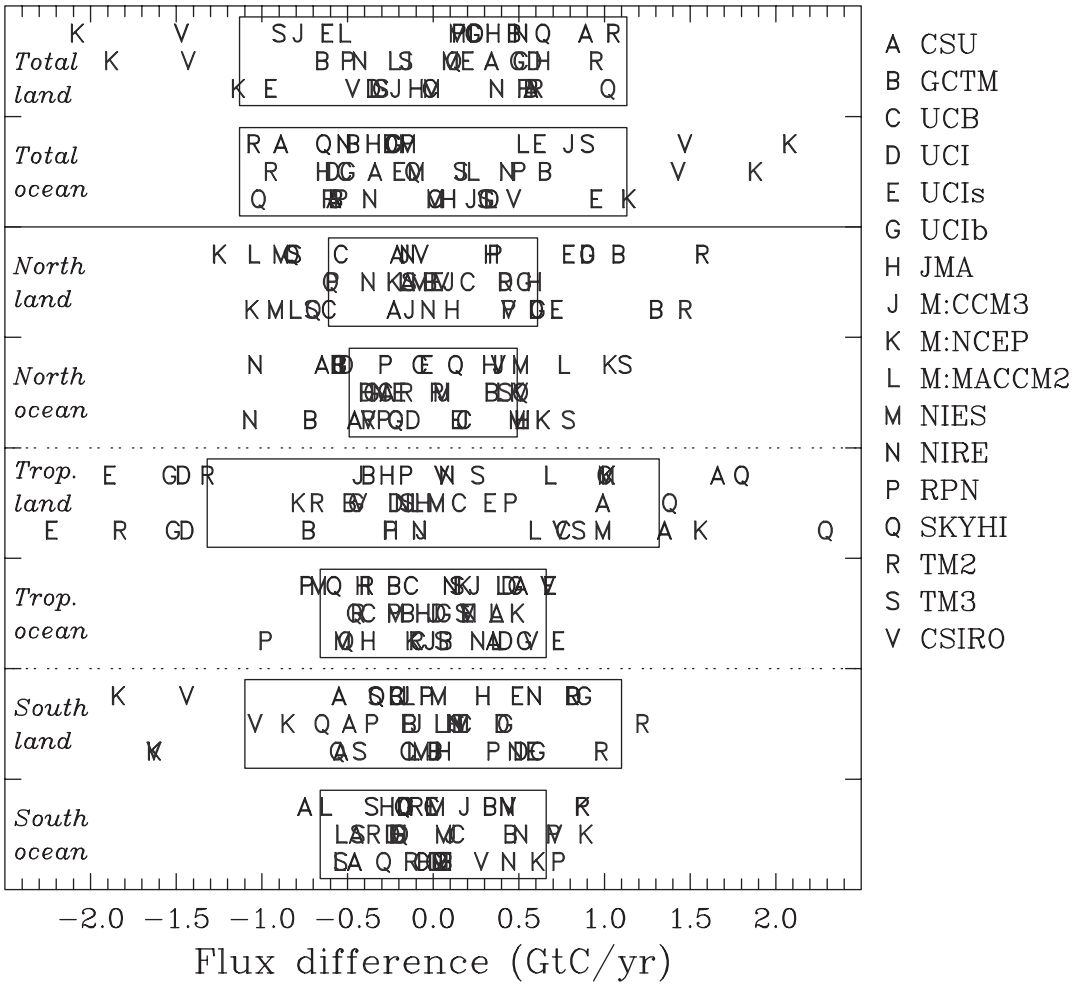

Figure 6. Aggregated posterior flux differences from the model mean for the control inversion (top row in each box), the 'No Rect' case (sensitivity test 3, middle row in each box) and the 'Zero Ocean' case (sensitivity test 5, bottom row in each box). The box represents the within-model uncertainty (1σ). Regional aggregation is as follows: North land (Boreal North America, Temperate North America, Europe, Boreal Asia, Temperate Asia),North ocean (North Pacific, Northern Ocean, North Atlantic), Tropical land (Northern Africa, Tropical Asia, Tropical America), Tropical ocean (West Pacific, East Pacific, Tropical Atlantic, Tropical Indian), South land (Southern Africa, Australasia, South America), South ocean (South Pacific, South Atlantic, South Indian, Southern Ocean).

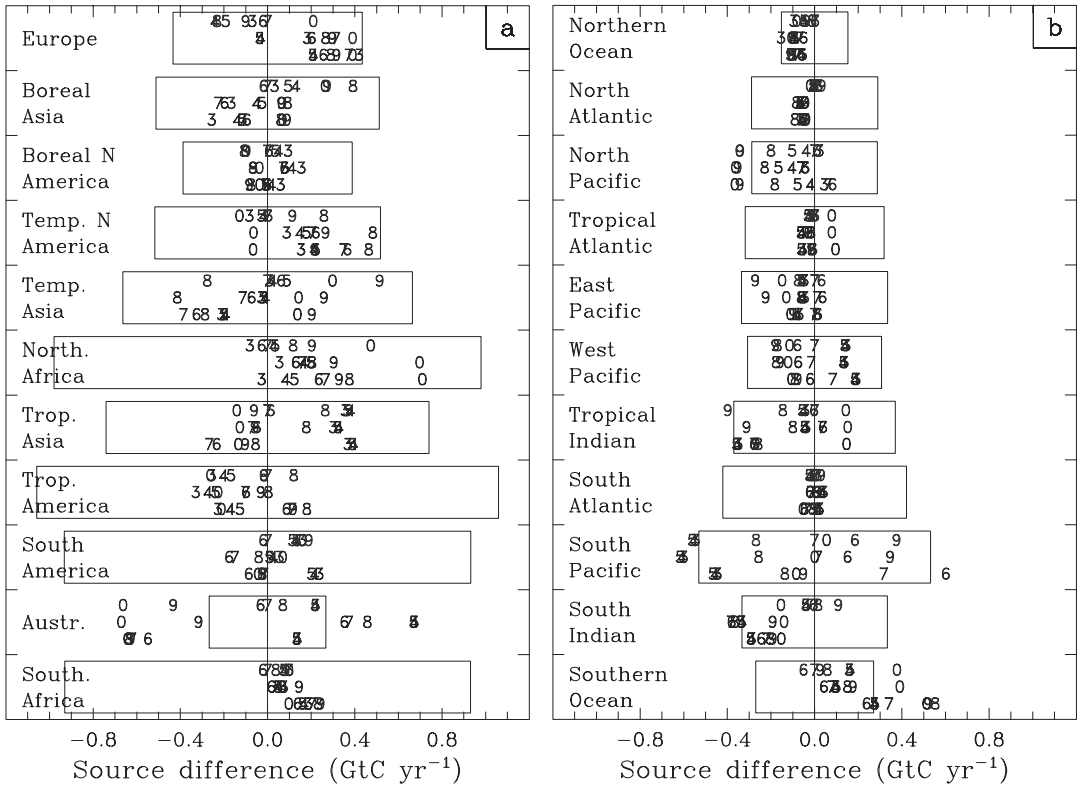

Figure 7. Difference in mean estimated source between the control inversion and inversions with different networks as indicated by the numbers for (a) land and (b) ocean regions. The regions are arranged approximately in their north-south order. The bottom row in each box is NOAA networks, the middle row is NOAA+CSIRO networks and the top row is ALL networks. The number indicates the record-completeness criterion: 100% (0), 90% (9), 80% (8), 70% (7), 60% (6), 50% (5), 40% (4), 30% (3). The control inversion is the ALL case with 70% criterion so the '7' in the top row always lies on the zero difference line. The box shows the magnitude of the within-model source uncertainty estimated in the control case.

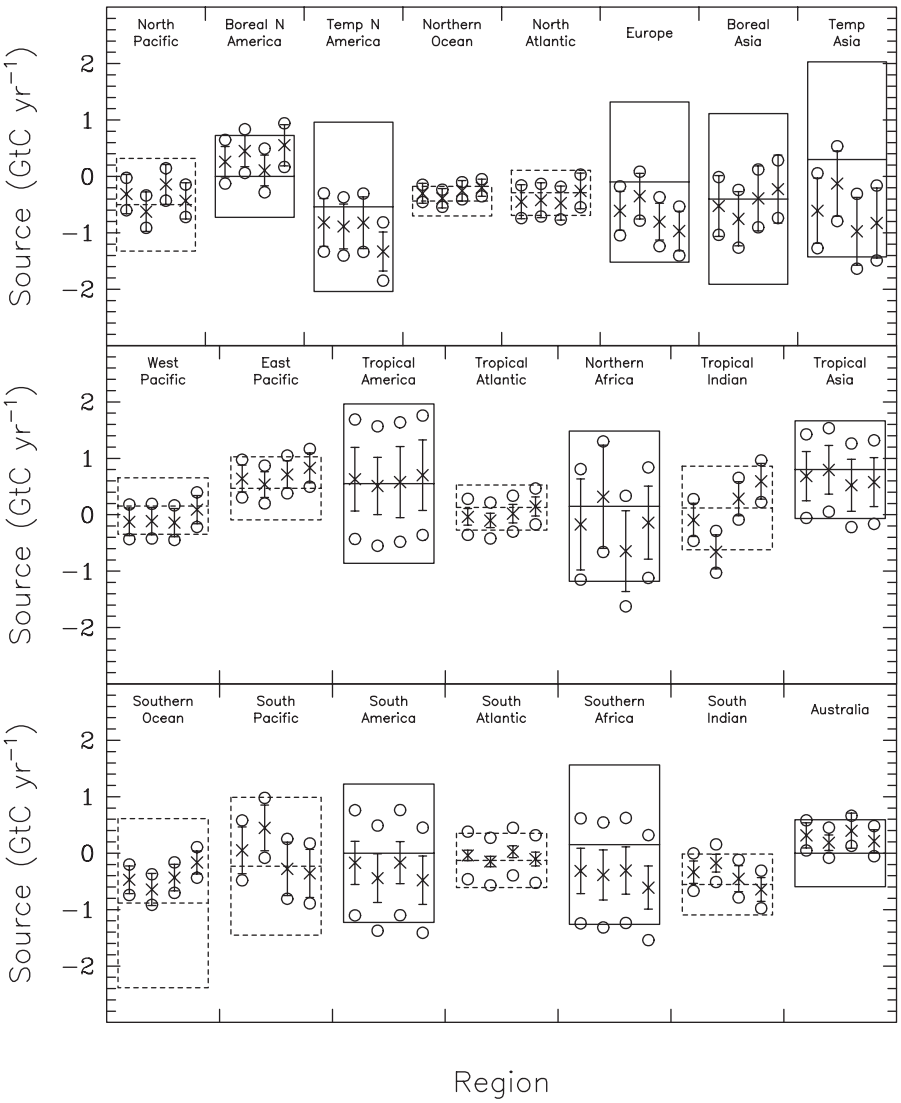

Figure 8. Model mean inversion results for all 22 basis regions using different data from different time periods. The leftmost value in each box is the control case 1992-1996, followed by 1995-1997, 1992-1994, and 1989-1991 respectively. Mean source estimates (including the background ocean ux es) are indicated by the x, mean within-model uncertainty by the o and between-model uncertainty (the standard deviation across model source estimates) by the bar. For each land (solid line) and ocean (dashed line) region, the boxes represent the prior source estimate (central horizontal line) and prior uncertainty. Regions are arranged to approximate their north-south and east-west relationship.

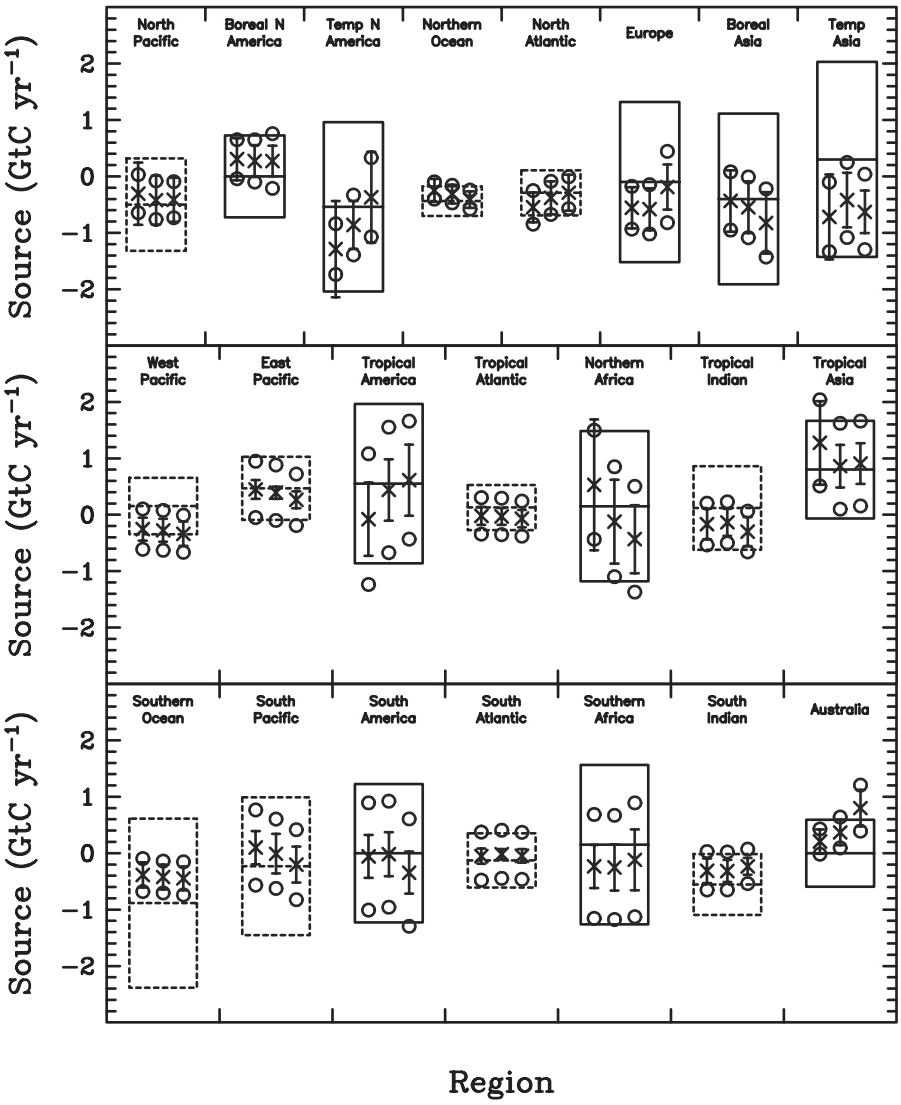

Figure 9. As Figure 8 but showing mean sources and uncertainties for three sets of inversions with different data selection strategies. Left is the 'nearest-grid' inversion, centre is the modied control inversion, right is the 'flask-like' inversion.

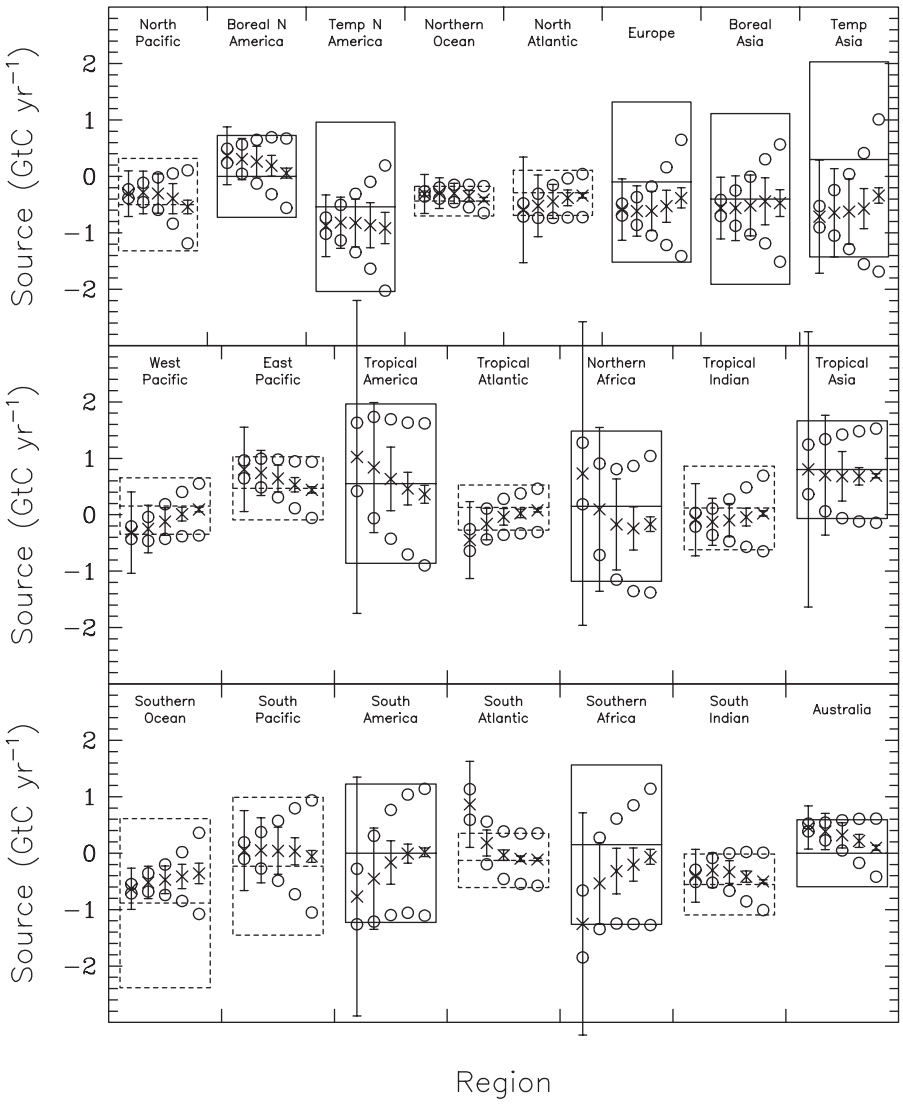

Figure 10. As Figure 8 but showing mean sources and uncertainties for Þve sets of inversions with scaled data uncertainties. The control data uncertainties were multiplied by 0.2 (far left), 0.5 (left), 2.0 (right), 5.0 (far right). The control inversion results are in the centre of each box.

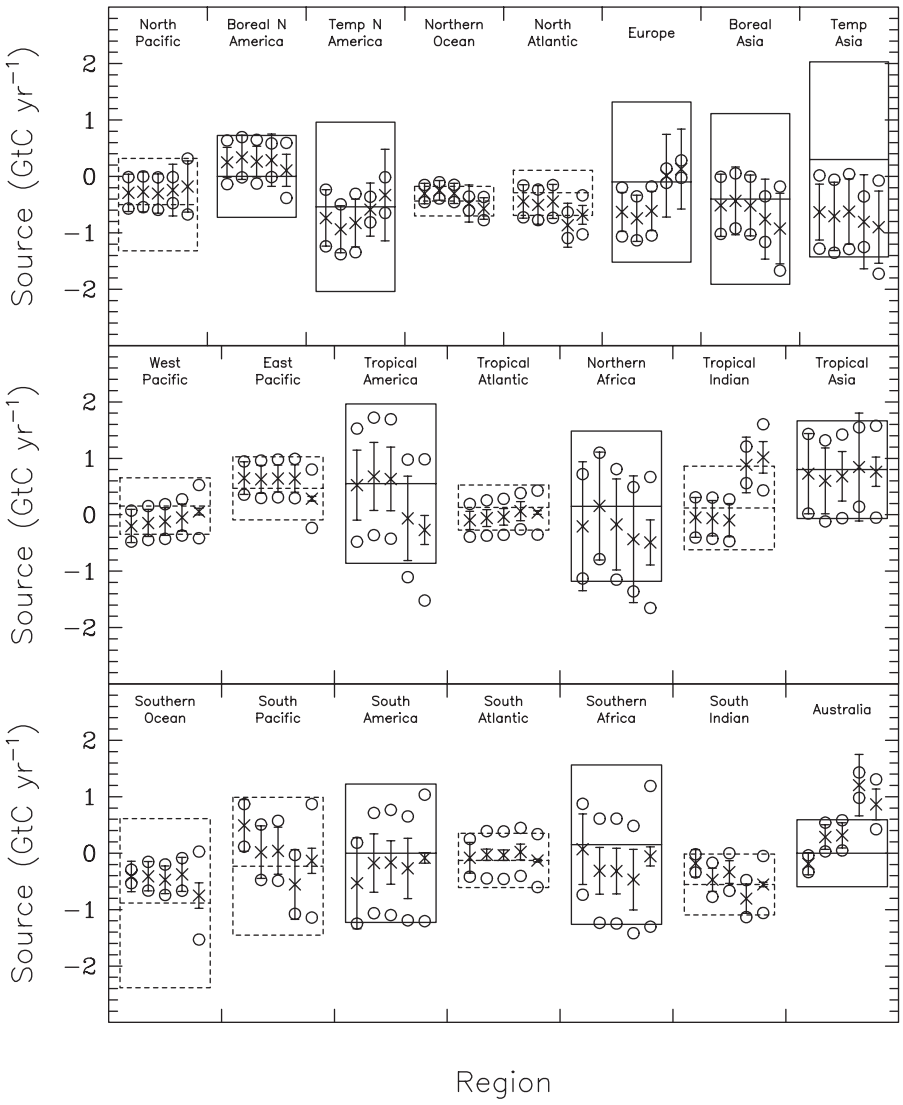

Figure 11. As Figure 8 but showing mean sources and uncertainties for Þve sets of inversions that used different spatial patterns of data uncertainty: no minimum (far left), no account of co-location (left), control (centre), constant 0.3 uncertainty (right), reversed distribution (far right).

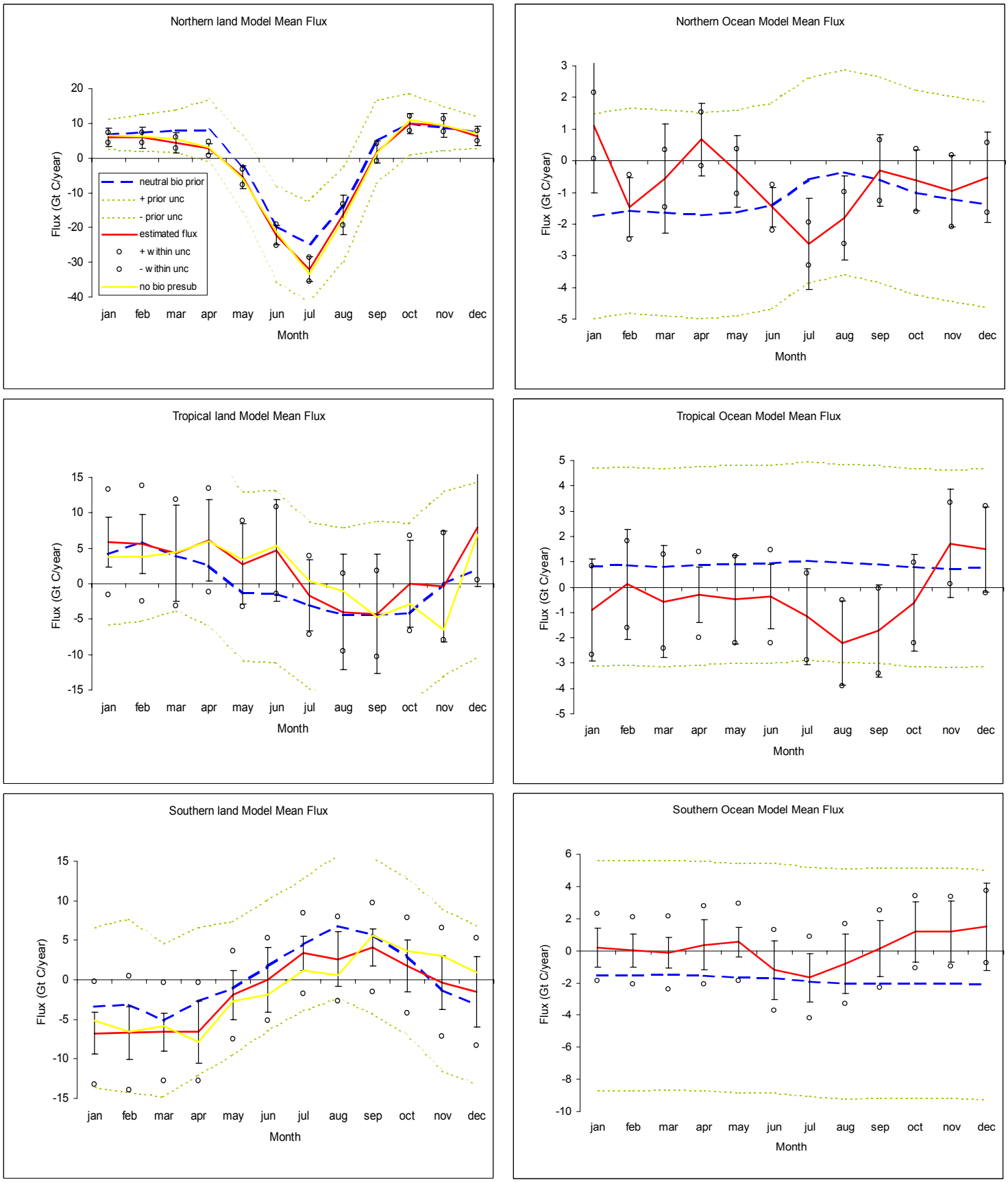

Figure 12. Model mean estimated flux (solid red), prior flux (dashed blue), prior uncertainties (dashed green) and posterior uncertainties (see figure 1 for explanation of uncertainty symbols) for aggregated land and ocean regions. Model mean estimated flux for inversion without neutral biosphere is given in yellow.

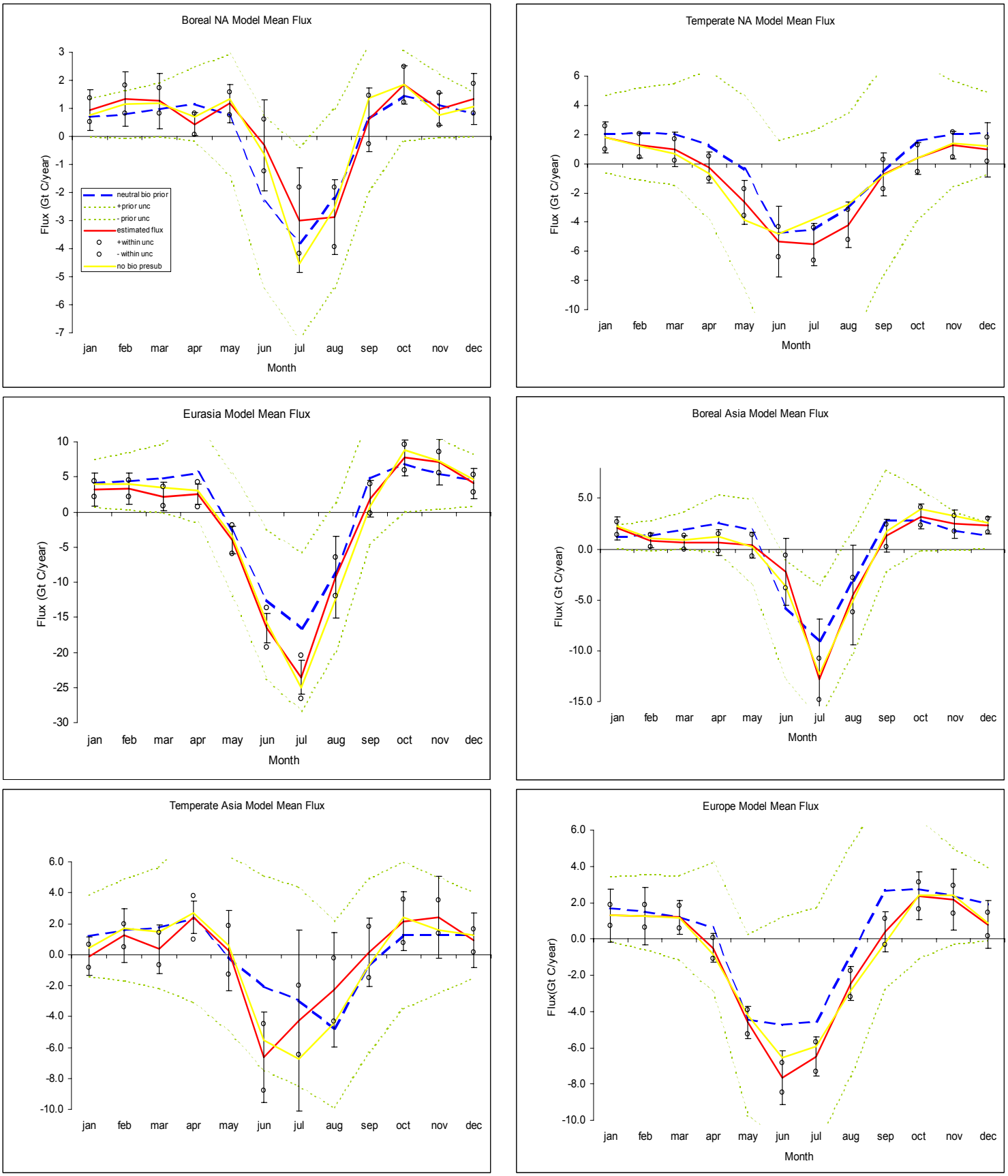

Figure 13. As in figure 12 but for disaggregated land and ocean regions.

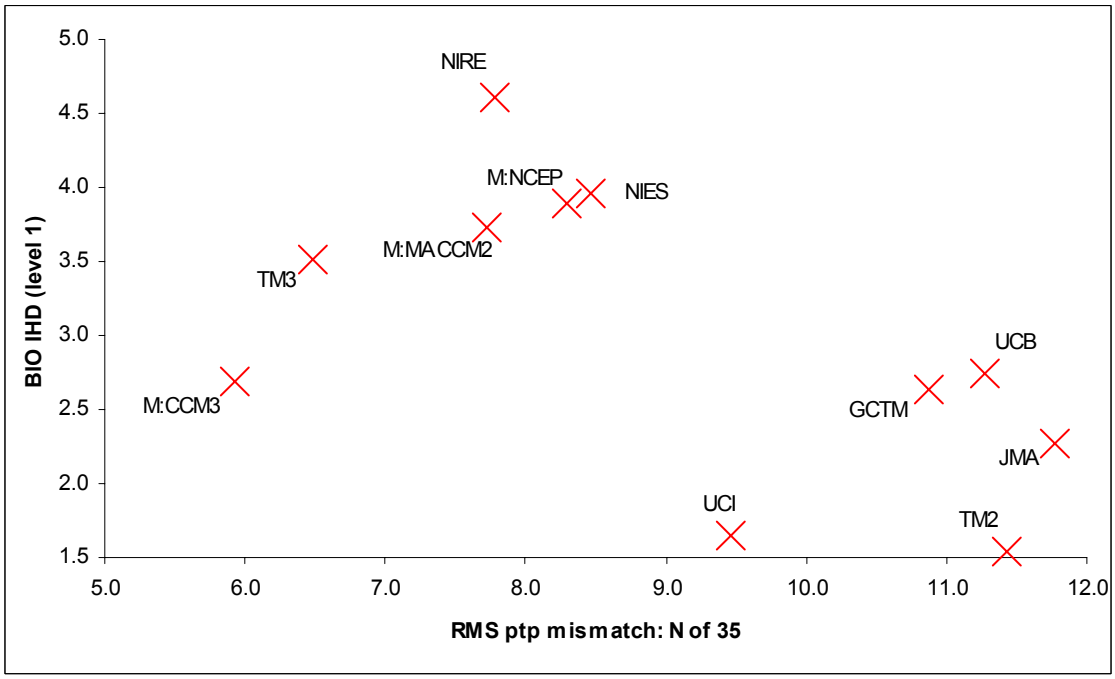

Figure 14. The annual mean neutral biosphere interhemispheric difference (ppm) versus the RMS maximum peak-to-peak mismatch for all stations north of 35 N latitude.